A PARTITION APPROACH FOR UNDERWATER EXPLOSION BASED ON SMOOTHED PARTICLE METHOD

A.M. ZHANG*, F.R. MING, X.Y. CAO

College of shipbuilding engineering
Harbin Engineering University
Harbin 150001, China
*E-mail: zhangaman@hrbeu.edu.cn

Key words: Fluid-structure interaction, underwater explosion, coupling, SPH shell, DAA$_2$

Abstract. As a Lagrangian particle method, smoothed particle hydrodynamics (SPH) has been applied into the problems of fluid-structure interaction (FSI) more and more. However, the transient fluid-structure interactions characterized by severe reactions and wide spreads are very expensive to be carried out with three-dimensional SPH method due to the approach of solid modeling, especially when the structure is subjected to the shock loads from mid-field or far-field, which is almost impossible to achieve. Therefore, based on the previous research, the coupled SPH-BEM method is put forward and applied to underwater explosion in this paper. The structure is modeled and solved with SPH method while the fluid boundary only required is coped with a boundary element method (BEM), the second-order doubly asymptotic approximations (DAA$_2$). The FSI method will reduce the elements of structures and fluid greatly so as to solve the problems of fluid-structure interactions feasibly and efficiently. The mid-plane of a plate only discretized into a layer of particles is taken as the study object in the SPH shell element and the related physical quantities is integrated in the thickness direction to capture the dynamic response of structures; the fluid boundary only discretized into a piece of boundary elements is employed in the BEM method to solve fluid dynamics based on the retarded potential equation; treatments of the coupled fluid-structure interface are made to satisfy the compatibility conditions and the messages related to motions and loads are well delivered. Finally, two standard examples are carried out to test the above algorithm.

1 INTRODUCTION

The transient FSI is always a troubling and headachy problem and is regarded as a hotspot issue [1-2]. Generally, the transient FSI process is a complicated and difficult one involving the fluid dynamics and structural responses, etc. The solutions of the FSI problems can be classified into two categories: the monolithic one and the partition one [3-8]. The differences between them are the structure and fluid solvers and the treatments of the coupled surface. The monolithic one [3-5] is a synchronous solver solving the structures and fluid simultaneously with the complexly coupled governing equations of structures and fluid, while for the partition one [6-8], it is asynchronous and the equations are uncoupled. The coupled surfaces of the partition one need to be imposed implicitly and yet it is satisfied automatically for the monolithic one. Though many numerical algorithms [9-13] have been raised, such as the method based on mesh as Finite Element Method (FEM), Spectral Element Method (SEM), BEM and the method based on meshless as Element Free Galerkin method (EFG) and

SPH, there is not a method singly coping with these difficulties completely. Accordingly, many FSI methods based on the partition approach emerge [6-8], including the SPH-FEM coupling, the FEM-BEM coupling, etc. The approach is featured by simplicity and good operability and thus has appealed many scholars. However, in the partition approach, the treatments of coupled surfaces are vital for the stability and accuracy of the coupled method. In this paper, the coupled SPH-BEM method based on the partition approach is proposed for the transient FSI problems.

In the coupled SPH-BEM method, the SPH shell is selected to discretize the thin structures via only a layer of particles; the fluid boundary is only needed and is discretized into a piece of polygonal elements, which will make the simulations of the mid- and far- field underwater explosion feasible and save the costs of the computation greatly. What's more, the coupled method will integrate the advantages of the above two methods and make the simulation of underwater explosion efficient: the SPH shell will provide the structural solver of nonlinearity and the BEM will act as the fluid dynamics solver of larger fluid domain. In the following, based on the previous studies of Zhang and Ming et al. [14], the SPH shell and the BEM method will be presented firstly, followed by the details of the coupled method and finally two examples will be carried out to test the above algorithm.

2   THE SPH SHELL METHOD

The SPH shell method is firstly proposed by Combescure et al. [15-16] and then studied by Ming et al. [17]. The SPH shell method devotes itself to solving two problems: stability and accuracy, which always exist in the traditional SPH method, especially when dealing with solid. The instability mainly comes from the stress instability including the tensile and compression instability which cannot be solved simultaneously as shown in many researches. The SPH shell method has taken many measures to overcome the instability, including the Lagrangian kernel function [18], total Lagrangian equation [19], stress point [20], conservative smoothing [21], artificial stress [22] and viscosity [23], etc. The poor accuracy is mainly from the traditional kernel function and the approximation method of itself, especially the boundary defects. The SPH shell method focuses on the approximation function of high accuracy, e.g. moving least square (MLS) function [24] and normalized SPH function (NSPH) [25], which satisfy the consistency of different orders.
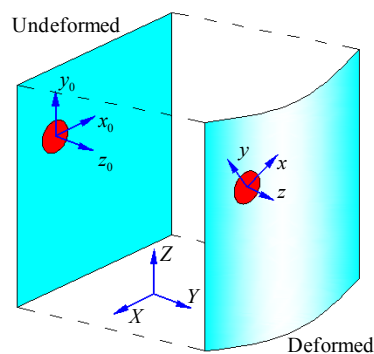

Figure 1: Three configurations of a SPH shell; the local configuration is defined by the normal of the shell and two orthogonal tangents

The SPH shell is only discretized into a layer of particles and the mid-plane is taken as the study object. Three configurations should be defined, namely, the global configuration, the initial local configuration and the current local configuration. The local configuration is defined with the two orthogonal tangents and the normal the shell, as shown in Figure 1. The MLS function and the total Lagrangian governing equation described in the initial configuration are selected as the approximation function and the approximation equation respectively. The position, the translational displacement of a given point in cross-section and the angular displacement of the shell's normal can be respectively noted as $\boldsymbol{x} = (x, y, z)^{\mathrm{T}}$, $\boldsymbol{u} = (u, v, w)^{\mathrm{T}}$, $\boldsymbol{\psi} = (\psi_x, \psi_y, 0)^{\mathrm{T}}$ in the local configuration and $\boldsymbol{X} = (X, Y, Z)^{\mathrm{T}}$, $\boldsymbol{U} = (U, V, W)^{\mathrm{T}}$, $\boldsymbol{\Psi} = (\Psi_x, \Psi_y, \Psi_z)^{\mathrm{T}}$ in the global configuration. The displacement in local configuration can be expressed as:

$$\begin{cases} u = u_m - z\psi_x \\ v = v_m - z\psi_y \ , \quad z \in [-t/2, t/2] \\ w = w_m \end{cases} \tag{1}$$

where the subscript 'm' indicates the quantities of mid-plane; t is the thickness of the shell.

The Green strain $\boldsymbol{E}$ described in the initial local configuration can be expressed by the gradient of displacement [19]:

$$\boldsymbol{E} = 0.5 \left[\nabla_0 \boldsymbol{u}_0 + (\nabla_0 \boldsymbol{u}_0)^{\mathrm{T}} + \nabla_0 \boldsymbol{u}_0 (\nabla_0 \boldsymbol{u}_0)^{\mathrm{T}} \right] = \boldsymbol{E}_C + \boldsymbol{E}_L(z) \tag{2}$$

the subscript '0' indicates the quantities in the initial configuration and the high-order nonlinear terms z^2 are ignored in the present shell model; $\boldsymbol{E}_C$ and $\boldsymbol{E}_L$ denote the constant and linear components respectively. According to the transformations of different configurations, the Almansi strain ε in the current local configuration turns to be:

$$\boldsymbol{\varepsilon}_C + \boldsymbol{\varepsilon}_L(z) = \boldsymbol{D} \cdot \boldsymbol{F}^{-\mathrm{T}} \cdot \boldsymbol{D}_0^{\mathrm{T}} \cdot (\boldsymbol{E}_C + \boldsymbol{E}_L) \cdot \boldsymbol{D}_0 \cdot \boldsymbol{F}^{-1} \cdot \boldsymbol{D}^{\mathrm{T}} \tag{3}$$

where $\boldsymbol{D}_0$ and $\boldsymbol{D}$ are orthogonal rotation matrices linking the initial and current local configuration with the global configuration respectively [17]; $\boldsymbol{F}$ is the gradient tensor standing for the structural deformation [19]. Considering the constitutive relation of elasticity or elastoplasticity in shell plane, the Cauchy stress $\boldsymbol{\sigma}_C = g(\boldsymbol{\varepsilon}_C)$ and $\boldsymbol{\sigma}_L(z) = g(\boldsymbol{\varepsilon}_L)$ can be drawn. $g(x)$ is the function of constitutive relation. Hence, the membrane force $\boldsymbol{C}$ and moment $\boldsymbol{L}$ in a unit length are:

$$\boldsymbol{C} = \int_{-t/2}^{t/2} \boldsymbol{\sigma}_C dz \ , \quad \boldsymbol{L} = \int_{-t/2}^{t/2} z\boldsymbol{\sigma}_L(z) dz \tag{4}$$

According to the properties of force, respectively the membrane force $\boldsymbol{\varLambda}$, the moment $\boldsymbol{\varOmega}$ and the transverse shear force $\boldsymbol{T}$ can be noted as:

$$\boldsymbol{\varLambda} = \left(C_{xx} \ C_{xy} \ C_{xz}; C_{yx} \ C_{yy} \ C_{yz}; C_{zx} \ C_{zy} \ 0 \right) \tag{5}$$

$$\boldsymbol{\varOmega} = \left(L_{xx} \ L_{xy} \ 0; L_{yx} \ L_{yy} \ 0; 0 \ 0 \ 0 \right) \tag{6}$$

$$\boldsymbol{T} = \left(C_{xz} \ C_{yz} \ 0 \right) \tag{7}$$

so the nominal force in the global configuration is:

$$\boldsymbol{\varLambda}_g = J\boldsymbol{F}^{-1}\boldsymbol{D}^{\mathrm{T}}\boldsymbol{\varLambda}\boldsymbol{D} \tag{8}$$

$$\boldsymbol{\varOmega}_g = J\boldsymbol{F}^{-1}\boldsymbol{D}^{\mathrm{T}}\boldsymbol{\varOmega}\boldsymbol{D} \tag{9}$$

$$T_g = J D^\mathrm{T} T \tag{10}$$

where $J = |F|$, the subscript 'g' indicates the quantities in the global configuration; thus the total Lagrangian formulas of SPH shell expressed by nominal force [19] are obtained:

$$\rho_0 t \ddot{U} = \nabla_0 \cdot \Lambda_g + Q_g \tag{11}$$

$$I_0 \ddot{\Psi} = \nabla_0 \cdot \Omega_g - T_g + M_g \tag{12}$$

where I_0 indicates the coefficient related to the rotation of particles; Q and M denote the external loads; '$\cdots$' is the second derivative versus time; thus, the discretized forms of the above total Lagrangian formulas are expressed as[26]:

$$\rho_0 t \ddot{U}_i^a = \sum_b \Lambda_{ij}^b N_{,X_{0j}}^{ab} + Q_i^a \tag{13}$$

$$I_0 \ddot{\Psi}_i^a = \sum_b \Omega_{ij}^b N_{,X_{0j}}^{ab} - T_i^a + M_i^a \tag{14}$$

herein, the superscript 'a' and 'b' denote a pair of interactional particle; the subscript 'i' indicates the coordinate direction; $N_{,X}$ equals $\partial N / \partial X$. Hence, the position and the angle can be updated by the time integration schemes and the explicit central difference scheme is adopted here, see [19]. Besides, the Rodrigue formula [27] is employed to rotate the normal.

3 THE DAA₂ METHOD

In the coupled FSI system, the pressure Q on the surface of structures can be categorized as the incident pressure Q_{inc} and the scattering pressure Q_{sca}. The incident pressure is always obtained from the propagation laws of the incident waves. As shown in Figure 2, it is a time-varying pressure at a spatial point x_j of the form [28]:

$$Q_{inc}(x_j, t) = Q_t(t - \frac{d_j - d_0}{c}) Q_x(x_j) \tag{15}$$

where

$$d_0 = \| x_s - x_0 \| \tag{16}$$

for planar waves,

$$d_j = |(x_j - x_s) \cdot (x_0 - x_s)| / \| x_s - x_0 \|, \quad Q_x(x_j) = 1 \tag{17}$$

However, the solution of the scattering pressure is always a challenge.
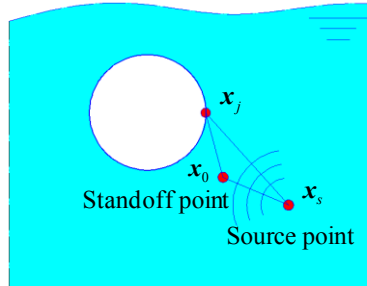

Figure 2: The propagation of incident waves

In this paper, the scattering pressure is solved with DAA₂. As a BEM method, it is appealing for the only requirement of the boundary discretization. The DAA₂ is first proposed

by Geers et al. [36-38] based on the principle of the retarded potential [29-30]:

$$\lambda\Phi(r_p,t) = -\iint_S \frac{1}{r_{pq}}\dot{\boldsymbol{u}}\left(r_q,t-\tau\right)\cdot\boldsymbol{n}_q dS_q - \iint_S \frac{\boldsymbol{r}_{pq}\cdot\boldsymbol{n}_q}{r_{pq}^3}\left[\Phi(r_q,t-\tau) + \frac{r_{pq}}{c}\dot{\Phi}(r_q,t-\tau)\right]dS_q \qquad (18)$$

where S is the FSI surface; $\boldsymbol{u}$ is the displacement of the FSI surface and the superscript ' $\cdot$ ' indicates the partial derivative versus time ; p and q represent two elements; Φ is the potential of velocity; r is the position; $\tau = r_{pq}/c$ is the retarded time; $\boldsymbol{n}_q$ is the unit normal at q pointing outward; λ is the three-dimensional angle. In the deducing of DAA$_2$, a linear assumption of the scattering pressure Q_{sca} (a component of $\boldsymbol{Q}_{sca}$) of boundary nodes is introduced, namely:

$$Q_{sca} = -\rho\dot{\Phi}_{sca} \qquad (19)$$

Therefore, the core of DAA$_2$, the discretized boundary approximate equation about scattering pressure of fluid can be derived [31]:

$$\boldsymbol{H}^{-1}\boldsymbol{G}\ddot{\boldsymbol{Q}}_{sca} + \rho c\dot{\boldsymbol{Q}}_{sca} + \rho c^2\boldsymbol{G}^{-1}\boldsymbol{H}\boldsymbol{Q}_{sca} = \rho c[\boldsymbol{H}^{-1}\boldsymbol{G}\ddot{\boldsymbol{u}}_{sca} + c\ddot{\boldsymbol{u}}_{sca}] \qquad (20)$$

herein, $\boldsymbol{H} = \iint_S f(r_q)\frac{\partial}{\partial n_q}\left(\frac{1}{|r_q - r_p|}\right)dS$, $\boldsymbol{G} = \iint_S \frac{f(r_q)}{|r_q - r_p|}dS$, $f(r)$ is a scalar function related to the position. The terms of $\ddot{\boldsymbol{u}}_{sca}$, $\ddot{\boldsymbol{u}}_{sca}$ on the right of equation (20) can be obtained through the treatments of the coupled surface, as shown in Section 4. In this way, through the numerical integration scheme, $\ddot{\boldsymbol{Q}}_{sca}$ and $\dot{\boldsymbol{Q}}_{sca}$ on the left of equation (20) can be expressed by $\boldsymbol{Q}_{sca}$ and thus $\boldsymbol{Q}_{sca}$ is solved.

4 THE COUPLED SPH-BEM METHOD FOR FSI

The coupled SPH-BEM method is a partition approach which is apt to model the fluid and the structure separately and operate modularly. Nevertheless, the SPH shell is a particle-based meshless method but the DAA$_2$ is a mesh-based method, so the treatments of the coupled surface are crucial for the SPH-BEM method. The mappings between the structure and the fluid at the coupled surface are various, including the boundary nodes corresponding to the SPH particle, see in Figure 3(a), the elements corresponding to the SPH particles, see in Figure 3(b), and other irregular correspondences, see in Figure 4. No matter what mapping schemes are employed, the treatments of the coupled surface are almost same. It is similar to the idea of the stress point in SPH shell: the SPH shell particles and the boundary nodes are put together and the MLS function is introduced to link them. Because the coupled model is only discretized into a layer of shell particles and a piece of boundary elements, the MLS function is constructed in the local configuration, which is defined by two orthogonal tangents and the normal of the coupled surface [14]. It is indeed a two-dimensional case. As for an SPH shell particle or a boundary node, the MLS function of itself is constructed by boundary nodes or SPH shell particles in its support domain, which is plotted in Figure 4, the radius of which is selected as 1.5 times of the characteristic length in the present research.

When the load information delivered from boundary nodes to SPH shell particles, the boundary nodes in the support domain of SPH shell particles will be used to construct the MLS function of SPH shell particles, and thus the load message carried by boundary nodes will be transformed to SPH shell particles; similarly, when the motion information delivered

from SPH shell particles to boundary nodes, the SPH shell particles in the support domain of boundary nodes will be used to construct the MLS function of boundary nodes, and thus the motion quantities of boundary nodes, such as displacement, velocity and so on, can be obtained from SPH shell particles [14]. Due to the consistency of the MLS function is completely satisfied and thus the information of the coupled surface will be well delivered, which is critical to the stability and accuracy of the coupled algorithm [14]. The flowchart of the coupled program is presented in Table 1.

○ SPH particle   ● Boundary node
(a)

○ SPH particle   ● Boundary node
(b)

○ SPH particle   ● Boundary node
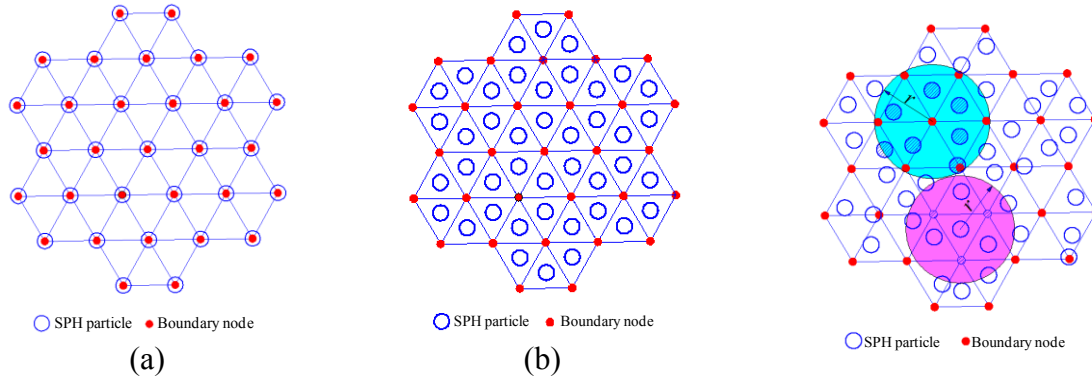
Figure 3: The mapping relation between SPH particles and boundary nodes; (a) SPH particles corresponding to boundary nodes, (b) SPH particles corresponding to boundary elements

Figure 4: The construction of the MLS function for SPH particles and boundary nodes in the approximation process

Table 1: The flow chart of the coupled program

(a) Initialize the model and parameters;
(b) Solving MLS function, containing the function used for SPH shell and the coupled surface;
(c) Solving the discretized boundary equation for fluid dynamics;
(d) Transforming the fluid dynamics to the external loads of SPH shell by MLS function;
(e) Solving the discretized total Lagrangian equation of SPH shell;
(f) Updating the position, velocity and so on of SPH shell;
(g) Updating the motion quantities of boundary nodes by MLS function;
(h) Judging the time to end the calculation or go to (c);

5   RESULTS AND DISCUSSIONS

To test the above algorithm, a FSI model of underwater explosion is established in the coupled way, as shown in Figure 5 (a). A cylinder with two spherical caps at the two ends is submerged in water and subjected to incident waves of underwater explosion, which is exponentially decaying with the peak of 1.57 MPa. The geometric parameters and the material parameters of the model are listed in Table 2. The shell model has a length of L, a radius of r and a thickness of t. The engineering material is employed with the elastic modules E, Possion ratio υ and the density ρ_s. The fluid field model has the same geometric

parameters as the shell model, but it has a density of ρ_w and a sound velocity of c. The whole model is discretized into 1983 SPH particles, 1981 stress points and 1981 four-node boundary elements.
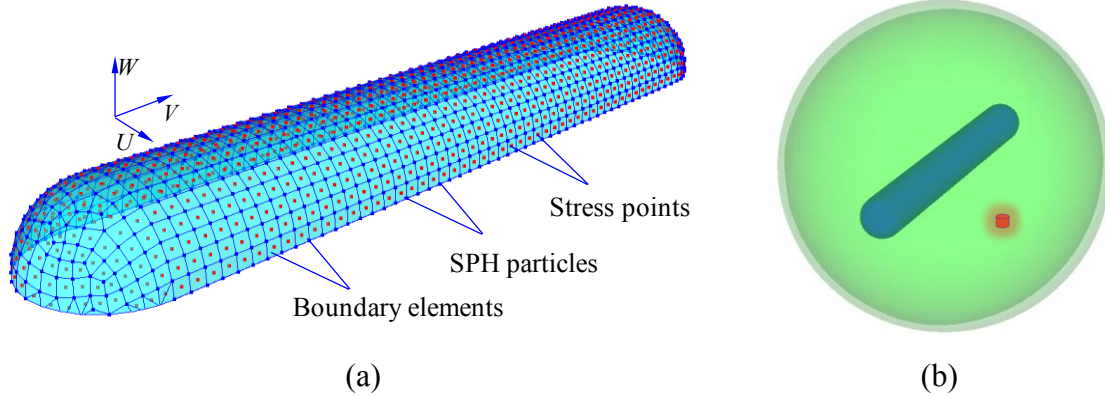

Figure 5: The calculation model of a cylinder with spherical caps; (a) the discretized SPH-BEM model, (b)the ABAQUS model

In order to carry out the comparative analyses, the FEM model, see in Figure 5 (b), and the analyses of the model are also performed with the software of ABAQUS. The four-node hex element and the four-node shell element are selected. The whole fluid field is discretized into 90272 hex elements and 1981 four-node shell elements for the shell model. The nodes of the shell model is positioned same as the SPH particles completely. The coupled acoustic-solid method and the nonreflecting boundary are applied in the analyses of ABAQUS.

Table 2: the parameters of the coupled model

L / m	r / m	t / m	E / GPa	υ	ρ_s / kg·m^{-3}	ρ_w / kg·m^{-3}	c / m·s^{-1}
1.2	0.1	0.01	210	0.3	7850	1026	1528

5.1 The cylinder with two spherical caps subjected to a longitudinal planar wave

Firstly, the coupled model subjected to a longitudinal planar wave is established. The incident wave fronts are perpendicular to the center axis of the model. The difficulties of the numerical model lie in the vibration of high-frequency along the center axis, which is related to the stability closely. The displacement of the head point subjected to the waves is shown in Figure 6. It is obvious that the displacement increases linearly within 1ms, and soon it starts to climb exponentially up to a stable value accompanied with vibrations of small amplitudes. However, the radial displacement of the midpoint of the model vibrates violently, see in Figure 7. When the incident waves have not arrived, the midpoint has a small displacement due to rigidity of the shell, but it starts to vibrate with a very high frequency under the impact the incident pressure. The amplitude of the displacement attenuates gradually and tends to be zero, which reveals the effects of the coupling. The typical deformation process of the shell is presented in Figure 8. It is obvious that the model vibrate severely.
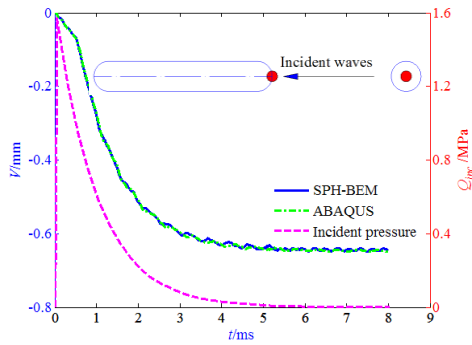
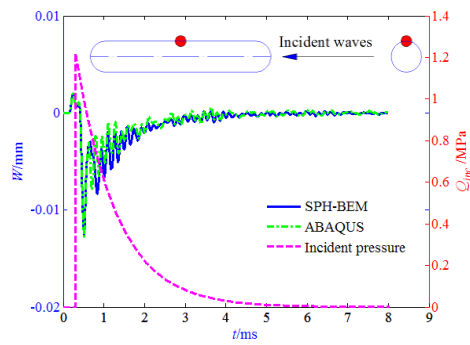**Figure 6:** The displacement and the incident pressure of the head point

Figure 7: The radial displacement and the incident pressure of the midpoint

Compared with the results of acoustic-structure approach, the results of the coupled SPH-BEM method show a good agreement. The vibration laws are in accordance with each other except some deviations of amplitudes, which may be from the treatments of the stability of different numerical methods. On the whole, the results are acceptable and appealing.
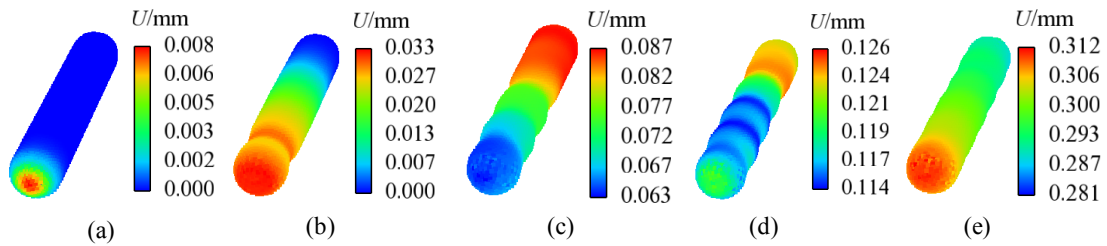

Figure 8: The typical deformation of the cylinder; (a) t=0.07ms, (b) t=0.25ms, (c) t=0.50ms, (d) t=0.70ms, (e) t=1.00ms

5.2 The cylinder with two spherical caps subjected to a transverse planar wave

Compared with the above model, the following model has a more complicated phenomenon. The same model is established and the same load is applied but the incident direction turns to be transverse. The difficulties of this model lie in the vibration of the shell body. The displacement of the head point in the incident direction is plotted in Figure 9. The displacement goes up linearly and then tends to be flat with several vibrations. The movement of the whole model is similar to a rigid body. However, the displacement of the pole point of the spherical cap vibrates violently under the impact of the incident pressure and decays to zero slowly, as shown in Figure 10. Moreover, the vibration of the upper point presented in Figure 11 is periodical with a large amplitude near zero. The typical deformation of the shell model is shown in Figure 12.
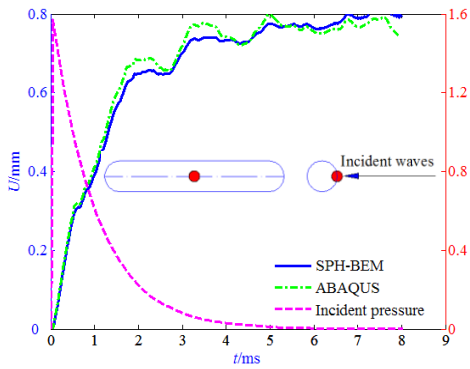
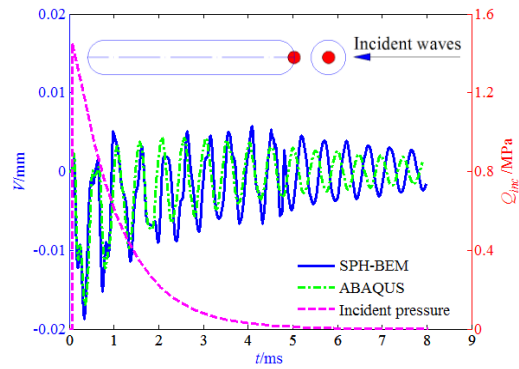**Figure 9:** The displacement and the incident pressure of the head point

Figure 10: The displacement and the incident pressure of the pole point of the spherical cap
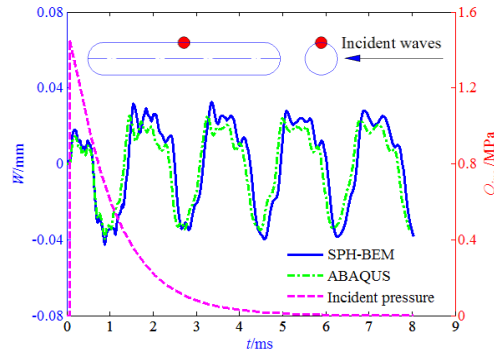

Figure 11: The displacement and the incident pressure of the upper point

Comparing the results of the above two methods, they agree well with each other except some time shifts and some deviations of amplitudes. Because of the fierce impact in the coupling process, the numerical integration scheme takes great effects on the synchronicity of the responses of the shell, which may be the main reason. Besides, the smoothing length of the shell model and the size of the domain to construct the MLS function are also the possible source of the deviations. To sum up, the results of the coupled model shows good feasibilities and accuracy, which verifies the effectiveness of the coupled algorithm proposed in this paper.
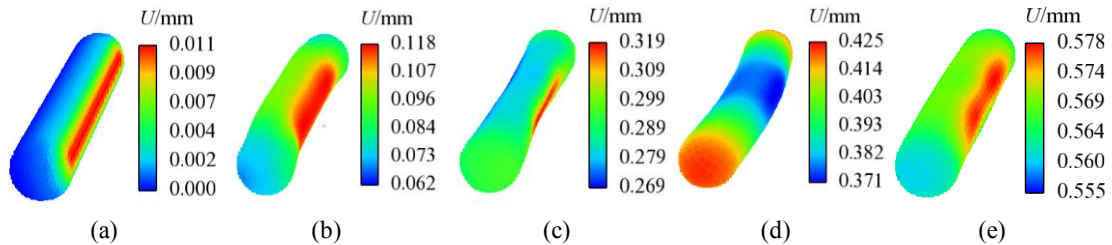

Figure 12: The typical deformation of the cylinder; (a) t=0.07ms, (b) t=0.25ms, (c) t=0.50ms, (d) t=1.20ms, (e) t=1.80ms

405

6   CONCLUSIONS

The coupled SPH-BEM method is proposed to deal with the transient FSI problems like underwater explosion based on the previous studies [14]. The SPH shell which is only discretized into a layer of particles is applied to provide a nonlinear structural solver in the coupled model; the DAA$_2$ method, a BEM approach, is employed to discretize the boundary of fluid field and treated as a solver of fluid dynamics of fluid field. In the coupled method, only a layer of shell particles and a piece of boundary elements are needed to model, which will make the simulations of FSI problems feasible and efficient. The coupled method has integrated the advantages of the above two methods.

This is a partition approach for FSI problem and thus the coupled surface has to be treated explicitly. The MLS function is introduced to impose the compatibility conditions of the FSI surface. Due to the consistency of the MLS function, the information is well delivered at the coupled surface. The final two examples of underwater explosion shows good agreements with those of FEM carried out with the acoustic-structure approach, which have verified the feasibility, the stability and the accuracy of the proposed method. It is a promising method.

REFERENCES

[1] Shin, Y.S. Ship shock modeling and simulation for far-field underwater explosion. *Comput. Struct.* (2004) **82**:2211-2219.

[2] Zhang, A.M., Zeng, L.Y., Cheng, X.D., Wang, S.P., Chen, Y. The evaluation method of total damage to ship in underwater explosion. *Appl. Ocean Res.* (2011) **33**: 240-251.

[3] Potapov, S., Maurel, B., Combescure, A., Fabis, J. Modeling accidental-type fluid-structure interaction problems with the SPH method. *Comput. Struct.* (2009) **87**: 721-734.

[4] Ryzhakov, P.B., Rossi, R., Idelsohn, S.R., Oñate, E. A monolithic Lagrangian approach for fluid-structure interaction problems. *Comput. Mech.* (2010) **46**: 883-899.

[5] Shao, J.R., Li, H.Q., Liu, G.R., Liu, M.B. An improved SPH method for modeling liquid sloshing dynamics. *Comput. Struct.* (2012) **100-101**: 18-26.

[6] Fernández-Méndez, S., Bonet, J., Huerta, A. Continuous blending of SPH with finite elements. *Comput. Struct.* (2005) **83**: 1448-1458.

[7] Yang, Q., Jones, V., McCue, L. Free-surface flow interactions with deformable structures using an SPH-FEM model. *Ocean Eng.* (2012) **55**: 136-147.

[8] Lee, C.J.K., Noguchi, H., Koshizuka, S. Fluid-shell structure interaction analysis by coupled particle and finite element method. *Comput. Struct.* (2007) **85**: 688-697.

[9] Hung, C.F., Hsu, P.Y., Hwang-Fuu, J.J. Elastic shock response of an air-backed plate to underwater explosion. *Int. J. Impact Eng.* (2005) **31**: 151-168.

[10] Klaseboer, E., Khoo, B.C., Hung, K.C. Dynamics of an oscillating bubble near a floating structure. *J. Fluids Struct.* (2005) **10**: 1-10.

[11] Sprague, M.A., Geers, T.L. A spectral-element/finite-element analysis of a ship-like structure subjected to an underwater explosion. *Comput. Methods Appl. Mech. Eng.* (2006)**195**: 2149-2167.

[12] Liu, M.B., Liu, G.R., Zong, Z., Lam, K.Y. Computer simulation of high explosive explosion using smoothed particle hydrodynamics methodology. *Comput. Fluids* (2003) **32**: 305-322.

[13] Zhang, A.M., Yang, W.S., Yao, X.L. Numerical simulation of underwater contact explosion. *Appl. Ocean. Res.* **(**2012**) 34**: 10-20.

[14] Zhang, A.M., Ming, F.R., Wang, S.P. Coupled SPHS-BEM method for transient fluid-structure interaction and applications in underwater shocks. *Appl. Ocean. Res.* (under review)

[15] Maurel, B., Combescure, A. An SPH shell formulation for plasticity and fracture analysis in explicit dynamics. *Int. J. Numer. Methods Eng.* (2008) **76**: 949-971.

[16] Caleyron, F., Combescur, A.e, Faucher, V., Potapov, S. Dynamic simulation of damage-fracture transition in smoothed particles hydrodynamics shells. *Int. J. Numer. Methods Eng.* (2012) **90**: 707-738.

[17] Ming, F.R., Zhang, A.M., Cao, X.Y. A robust shell element in meshfree SPH method. *Acta Mechanica Sinica* (2013) **29**: 241-255.

[18] Belytschko, T., Rabczuk, T., Xiao, S.P. Stable particle methods based on Lagrangian kernels. *Comput. Methods Appl. Mech. Eng.* (2004) **193**: 1035-1063.

[19] Belytschko, T., Liu, W.K., Moran, B. *Nonlinear Finite Elements for Continua and Structures*. John Wiley and Sons Ltd, New York,(2000).

[20] Dyka, C.T., Randles P.W., Ingel, R. P. Stress points for tensile instability. *Int. J. Numer. Methods Eng.* (1997) **40**:2325-2341.

[21] Randles, P.W., Libersky, L.D. Smoothed particle hydrodynamics: some recent improvements and applications. *Comput. Methods Appl. Mech. Eng.* (1996) **139**:375-408.

[22] Gray, J.P., Monaghan, J.J. SPH elastic dynamics. *Comput. Methods Appl. Mech. Eng.* (2001) **190**:6641-6662.

[23] Monaghan, J.J, Gingold, R.A. Shock simulation by the particle method SPH. *J. Comput Phys.* (1983) **52**: 374-389.

[24] Dilts, G.A. Moving least squares particle hydrodynamics-I: consistency and stability. *Int. J. Numer. Methods Eng.* (1999) **44**: 1115-1155.

[25] Randles, P.W., Libersky, L.D. Normalized SPH with stress points. *Int. J. Numer. Methods Eng.* (2000) **48**: 1445-1462.

[26] Liu, G.R., Liu, M.B. *Smoothed particle hydrodynamics: a meshfree particle method*. World Scientific, Singapore, (2003).

[27] Betsch, P., Menzel, A., Stein, E. On the parameterization of finite rotations in computational mechanics. A classification of concepts with application to smooth shells. *Comput. Methods Appl. Mech. Eng.* (1998) **155**: 273-305.

[28] Hibbitt, Karlsson and Sorensen, Inc., ABAQUS Theory Manual (version 5.4), Pawtucket, (2004).

[29] Huang, H., Everstine, G.C., Wang, Y.F. Retarded potential techniques for the analysis of submerged structures impinged by weak shock waves. *Comput. Methods Fluid Struct. Interact. Probl.* (1977) **26**: 83-93.

[30] Mitzner, K.M. Numerical solution for transient scattering from a hard surface-retarded potential technique. *J. Acoust. Soc. Am.* (1967) **42**: 391-397.

[31] Dyka, C.T., Ingel, R.P. Transient fluid-structure interaction in naval applications using the retarded potential method. *Eng. Anal. Bound. Elem.* (1998) **21**: 245-251.